ORIGINAL RESEARCH

Correlations between Perfusion MR Imaging Cerebral Blood Volume, Microvessel Quantification, and Clinical Outcome Using Stereotactic Analysis in Recurrent High-Grade Glioma

L.S. Hu
J.M. Eschbacher
A.C. Dueck
J.E. Heiserman
S. Liu
J.P. Karis
K.A. Smith
W.R. Shapiro
D.S. Pinnaduwage
S.W. Coons
P. Nakaji
J. Debbins
B.G. Feuerstein
L.C. Baxter

BACKGROUND AND PURPOSE: Quantifying MVA rather than MVD provides better correlation with survival in HGG. This is attributed to a specific "glomeruloid" vascular pattern, which is better characterized by vessel area than number. Despite its prognostic value, MVA quantification is laborious and clinically impractical. The DSC-MR imaging measure of rCBV offers the advantages of speed and convenience to overcome these limitations; however, clinical use of this technique depends on establishing accurate correlations between rCBV, MVA, and MVD, particularly in the setting of heterogeneous vascular size inherent to human HGG.

MATERIALS AND METHODS: We obtained preoperative 3T DSC-MR imaging in patients with HGG before stereotactic surgery. We histologically quantified MVA, MVD, and vascular size heterogeneity from CD34-stained 10-μm sections of stereotactic biopsies, and we coregistered biopsy locations with localized rCBV measurements. We statistically correlated rCBV, MVA, and MVD under conditions of high and low vascular-size heterogeneity and among tumor grades. We correlated all parameters with OS by using Cox regression.

RESULTS: We analyzed 38 biopsies from 24 subjects. rCBV correlated strongly with MVA ($r = 0.83$, $P < .0001$) but weakly with MVD ($r = 0.32$, $P = .05$), due to microvessel size heterogeneity. Among samples with more homogeneous vessel size, rCBV correlation with MVD improved ($r = 0.56$, $P = .01$). OS correlated with both rCBV ($P = .02$) and MVA ($P = .01$) but not with MVD ($P = .17$).

CONCLUSIONS: rCBV provides a reliable estimation of tumor MVA as a biomarker of glioma outcome. rCBV poorly estimates MVD in the presence of vessel size heterogeneity inherent to human HGG.

ABBREVIATIONS: DSC = dynamic susceptibility-weighted contrast-enhanced; GBM = glioblastoma multiforme; Gd = gadolinium; HGG = high-grade glioma; MION = monocrystalline iron oxide nanocompounds; MVA = microvessel area; MVD = microvessel density; OS = overall survival; rCBV = relative cerebral blood volume

Although the degree of angiogenesis in glioma generally correlates with malignant potential, histologic outcome studies have shown that the specific method of quantifying angiogenesis can greatly impact the ability to predict survival.[1-10] Most glioma studies have measured angiogenesis by using vessel number counts or MVD.[11-14] Both precedent and the relative ease of MVD calculation have made this technique a logical first choice to study outcome; however, while MVD shows good predictive power for non–central nervous system tumors, the correlation with glioma survival has been marginal at best.[1-6]

Received December 30, 2010; accepted after revision May 9, 2011.

From the Departments of Radiology (L.S.H.) and Biostatistics (A.C.D.), Mayo Clinic, Phoenix/Scottsdale, Arizona; Department of Neuropathology (J.M.E., S.W.C.), Keller Center for Imaging Innovation (L.S.H., S.L., J.P.K., D.S.P., J.D., L.C.B.) and Departments of Neuroradiology (J.E.H., J.P.K.), Neurosurgery (K.A.S., P.N.), and Neurology (W.R.S., B.G.F.), Barrow Neurological Institute—St. Joseph's Hospital and Medical Center, Phoenix, Arizona; and Department of Radiation Physics (D.S.P.), University of California, San Francisco, San Francisco, California.

This work was supported, in part, by the Barrow Neurological Foundation, Phoenix, Arizona (B.G.F., L.C.B.), Bruce T. Halle Family Foundation (B.G.F.), Arizona Biomedical Research Commission (L.S.H.), and Mayo Clinic Foundation (L.S.H.).

Please address correspondence to Leland S. Hu, MD, Department of Radiology, Mayo Clinic, 13400 E Shea Blvd, Scottsdale, AZ 85259; e-mail: hu.leland@mayo.edu

http://dx.doi.org/10.3174/ajnr.A2743

Specific characteristics of glioma angiogenesis are likely to account for the poor correlations with survival. HGGs are often characterized as having large-lumen microvessels that are few in number, large in area, and linked with aggressive behavior and poor prognosis.[4,6-8] These large-lumen microvessels can be composed of either a single lumen or multiple lumina, the latter having a "glomeruloid" appearance that is a histologic hallmark of grade IV tumors. MVD poorly characterizes the morphometric complexity of these large-lumen microvessels, because area and number are often inversely related.[1,4,6-8,14,15] In contrast, the MVA of the tumor vessels may provide a more salient clinical biomarker of glioma outcome. This assertion is supported by studies showing that MVA correlates more strongly with survival compared with MVD, even in tumors with similar histologic grades.[1,4,8-10] Despite this evidence, histologically quantifying MVA remains a research tool because the technique is time-consuming, labor-intensive, and thus impractical for routine clinical use.[6,7]

For >2 decades, DSC-MR imaging has been used to study glioma angiogenesis.[16-21] On the basis of the indicator dilution theory, DSC-MR imaging calculates rCBV to estimate tissue blood volume.[18,21,22] Because DSC-MR imaging is semiautomated, it offers advantages of speed and convenience that

overcome limitations of histologic vessel quantification. Because measurements can also be performed serially and noninvasively without surgical biopsy, DSC-MR imaging has the potential to lower cost, morbidity, and sampling error to better provide measures of outcome as well as treatment efficacy in patients with glioma. The clinical translation of DSC-MR imaging as a feasible alternative to histologic quantification requires correlations between rCBV, MVD, and MVA. To date, nearly all DSC-MR imaging correlative data are from animal models by using only MVD.[21,23-27] Although MVA likely represents a more clinically relevant parameter,[1,4,6-10] no human studies have been done and only 1 group has reported MVA correlation with rCBV in the rat 9L gliosarcoma model.[22,28]

Basing the clinical translation of DSC-MR imaging primarily on animal data has several distinct limitations. Animal models often lack the broad variations in vessel growth pattern and size that are observed in human HGG,[6-8,21,22,29] and it is unclear how the heterogeneity of human tumors impacts rCBV correlations with MVD and MVA. Additionally, large-area vessels in human HGG cause MVD and MVA to be inversely related[6-10]; this feature would directly challenge the consensus from animal studies that rCBV correlates well with both measures.[21-28] Finally, the rationale for using rCBV to predict glioma outcome has not been reconciled with extensive clinical data comparing histologically derived MVD and MVA with survival. Specifically, whether rCBV more strongly reports MVD versus MVA directly impacts the utility of rCBV as a clinical predictor of glioma outcome.[4,6-10] That these relationships are currently unproved in humans might explain why DSC-MR imaging has not yet gained significant traction as a part of clinical standard of care, with the exception of select academic institutions.[30]

To address these issues, we present data from a pilot study correlating localized coregistered rCBV with histologically derived MVD and MVA from stereotactic biopsies in human HGG. We hypothesized that rCBV would show stronger correlation with tissue MVA compared with MVD due to vascular patterns that cause vessel size heterogeneity. Similarly, we hypothesized that rCBV and MVA would show similar correlations with survival in a cohort of patients with HGG, whereas MVD would not. Thus, our aims in this study were the following: 1) to compare the strength of rCBV correlation with MVD and MVA, 2) to describe how vascular heterogeneity (ie, size variation) inherent in human HGG impacts these correlations; and 3) to investigate the associations between rCBV, MVD, and MVA as biomarkers of survival.

Materials and Methods

Subject Recruitment

We recruited patients with previous HGG who were to undergo new operations. We studied them during preoperative imaging performed for the stereotactic surgery procedure. We documented previous treatment (including chemoradiation therapy and/or previous surgical resection) and excluded subjects with an estimated glomerular filtration rate <60 mg/min/1.72 m^2. We obtained approval from the institutional review board and written informed consent from each subject.

Preoperative DSC-MR Imaging Protocol

We used the same 3T MR imaging magnet (Sigma HDx; GE Healthcare, Milwaukee, Wisconsin) for all patients. All imaging was performed within 1 day of surgery. An intravenous injection of 0.1 mmol/kg of Gd-based contrast agent (gadodiamide or gadobenate dimeglumines, preload dose) was administered before DSC-MR imaging on the basis of a previously published optimized protocol.[31,32] The DSC-MR imaging was performed by using a 0.05-mmol/kg Gd-agent bolus delivered at a rate of 3–5 mL/s. This dosage, at high field strength, provides strong signal intensity to noise while minimizing patient contrast load.[33,34] The DSC-MR imaging sequence parameters were the following: gradient-echo echo-planar imaging with TR/TE/flip angle, 1500–2000 ms/20 ms/60°; FOV, 24 × 24 cm; matrix, 128 × 128; 5-mm section; no intersection gap. The total Gd agent dose was 0.15 mmol/kg of body weight.

Preoperative Stereotactic Anatomic Dataset

3T T1-weighted spoiled gradient-echo stereotactic MR imaging datasets (TI/TR/TE, 300 ms/6.8 ms/2.8 ms; matrix, 320 × 224; FOV, 26 cm; section thickness, 2 mm) were obtained before and after DSC-MR imaging to use for neuronavigation during surgical resection and biopsy sampling.

Intraoperative Tissue Specimen Collection

Each neurosurgeon collected 2–3 tissue specimens from each tumor by using stereotactic surgical localization, following the smallest possible diameter craniotomies to minimize brain shift.[34-36] We chose not to use maximum or minimum rCBV values to guide biopsy targeting, to avoid biasing the correlation between rCBV, MVA, and MVD. Instead, biopsy targets were collected by using standard clinical criteria, such that specimens were collected in pseudorandom fashion from different poles of the enhancing lesion periphery while avoiding any necrotic regions. Biopsies were performed without knowledge of the DSC-MR imaging analyses. The locations of the biopsy sites and the neuronavigational coordinates were recorded at the time of surgical tissue collection as screen captures and were later coregistered with the MR imaging datasets to enable localized measurement of rCBV at the sites for each corresponding tissue sample. Multiple biopsy targets in the same patient were separated by a minimum of 2 cm. The neurosurgeon visually validated stereotactic imaging locations with corresponding intracranial anatomic landmarks, such as vascular structures and ventricle margins, before recording specimen locations.

Coregistration of Stereotactic and DSC-MR Imaging Datasets

Stereotactic and DSC-MR imaging were transferred to an off-line Linux-based workstation for rigid-body coregistration by using statistical parametric mapping (SPM5, Wellcome Department of Imaging Neuroscience, University College London, UK). DSC-MR imaging coregistration enabled region-of-interest placement for rCBV calculation within previously recorded stereotactic locations of corresponding surgical tissue specimens, as previously described.[33-35] All regions of interest were also inspected to ensure exclusion of visible large vessels.

DSC-MR Imaging Data Postprocessing and rCBV Calculation

DSC-MR imaging was analyzed by using an in-house Matlab-based program (MathWorks, Natick, Massachusetts) based on previously

published methods.[18,31,32,34] In short, we generated whole-brain CBV maps by integrating the first-pass $\Delta R2^*(t)$, using baseline subtraction to correct residual T2/T2*-weighted effects.[31,32] Following CBV normalization to contralateral normal gray and white matter as previously described,[34] we calculated mean rCBV for each tissue specimen from a 3 × 3 voxel (~0.8 cm^2) region of interest centrally placed within corresponding stereotactic locations. All analyses were performed without knowledge of tissue analysis.

Tissue Specimen Preparation and Histopathologic Diagnosis

All stereotactic biopsy specimens were fixed in 10% formalin and paraffin-embedded. CD34 immunohistochemistry was performed on 10-μm sections by using the Ventana Nexus immunostainer (Ventana Medical Systems, Tucson, Arizona). A prediluted monoclonal primary antibody (Mouse Anti-Human CD34, clone QBEnd/10, Ventana Medical Systems) was used with standard cell conditioning. The reaction product was visualized with diaminobenzidine. Negative control sections were processed identically with omission of the primary antibodies.[5,9] Corresponding sections were stained with hematoxylin-eosin per standard protocol. Specimens were diagnosed histologically according to the 2007 World Health Organization classification.[37]

Tissue Microvascular Parameter Quantification

Whole-section slides from each specimen were imaged and digitized by using an Axiovert 200M light microscope, Achroplan 20x Objective (Zeiss, Gottingen, Germany) and AxioVision Mosaix 4.8 (Zeiss). Whole-section quantitative microvascular analysis was performed by using the computer-assisted image analysis software AxioVision Automeasure 4.8 (Zeiss). Microvessel parameters were defined as previously described on the basis of CD34-stained profiles, as per the clinical protocol at our institution as well as techniques from multiple previous studies.[1,6,7,10,22] The mean smallest microvessel diameter was determined by using the ferret minimum function. The total area (square micrometers) of each section was also calculated and used to normalize respective microvascular parameters. Tissue analyses were supervised by 2 neuropathologists.

Statistical Analysis

We performed Pearson correlations between rCBV and microvascular parameters for all corresponding stereotactic biopsy samples, as demonstrated in Fig 1. We chose to perform linear correlations based on prior reports, which would facilitate the comparison of correlations from our study with those previously performed.[22,38] For clinical outcome analyses, we determined OS from the date of surgery to death for those patients who had died at the time of analysis. For each patient, rCBV, MVA, and MVD were determined across biopsy locations, and the maximum values (1 value per patient for each variable) were correlated with OS by using Cox regression survival analyses for all patients. The Cox regression analysis takes into account follow-up for all patients, not just for outcomes from which patients died. Patients who have not died contribute data until their last date known to be alive. To assess the influence of tumor grade (III or IV), we compared rCBV, MVA, and MVD between grade III and grade IV tumor samples by using the Fisher exact test. We also performed a Cox regression analysis, comparing tumor grade with OS. A biostatistician performed all analyses, and statistical significance was indicated by $P < .05$.

Results

Study Subjects and Tissue Specimens

We enrolled 27 subjects and collected a total of 75 tissue specimens, of which 54 contained sufficient tissue for both histopathologic diagnosis and microvascular quantification. Three samples were excluded due to poor CD34 staining quality, primarily seen as diffuse background staining. Also, 13 samples were diagnosed as having radiation effect without evidence of tumor and were therefore excluded. Final analyses were based on 38 HGG tissue specimens from 24 patients containing either grade III ($n = 17$) or grade IV ($n = 21$) tumor. The average tissue specimen volume was approximately 0.2 cm^3 with an average tissue cross-sectional area of 1.61 × $10^7 \mu m^2$. All patients had undergone previous surgical diagnosis for their primary tumor. The Table summarizes the original histopathologic diagnosis and the type and timing of prior chemotherapy and radiation treatments. In our study, the average postprocessing time for rCBV calculation was approximately 5 minutes, compared with approximately 45 minutes for histologic multiparametric vascular quantification. One grade III tumor sample demonstrated glomeruloid vessels. Because this patient received prior multimodality therapy (including radiation), the presence of glomeruloid vessels could not be entirely attributed to malignant progression; thus, on the basis of clinical diagnostic criteria at our institution by 2 board-certified neuropathologists, the tumor was not histopathologically upstaged to grade IV but rather maintained as grade III. There were no significant differences in rCBV ($P = .22$), MVA ($P = .16$), or MVD ($P = .42$) between grade III and grade IV tumor samples.

rCBV Correlation with MVA and MVD

Within the entire specimen group ($N = 38$), the mean MVA value was 0.0735 ± 0.062 with a range of 0.008–0.26 and the mean MVD value was 8.40E-4 ± 1.11E-3 μm^{-2} with a range of 5.07E-5–4.62E-3. The mean rCBV value was 1.49 ± 0.97 with a range from 0.38 to 4.64. rCBV correlated strongly with MVA ($r = 0.83$; $P < .001$; 95% confidence interval, $r = 0.69$–0.90). Measures of rCBV weakly correlated with MVD over the entire group ($N = 38$, $r = 0.32$; $P = .05$; 95% confidence interval, $r = 0.00$–0.58). Confidence intervals for rCBV correlations between MVA and MVD did not overlap. To test for possible intrasubject grouping effects of multiple tissue samples collected from a single subject, we performed a bootstrap analysis in which rCBV/MVA correlations were computed with random selection of 1 specimen per subject. The correlation remained consistent with the original analysis (average $r = 0.78$, standard error = 0.002).

Effect of Heterogeneity of Vascular Size on rCBV Correlation with Microvessel Area and Number

The rCBV correlation with MVD in our study differed from that of previous animal reports. To explain this difference, we examined the variation in vascular size within tissue samples. We postulated that because heterogeneity of vascular size is more commonly observed in human HGG than in animal models, greater heterogeneity might negatively impact the rCBV correlation with MVD in our dataset. To test this effect, we separated specimen sections into subgroups based on a

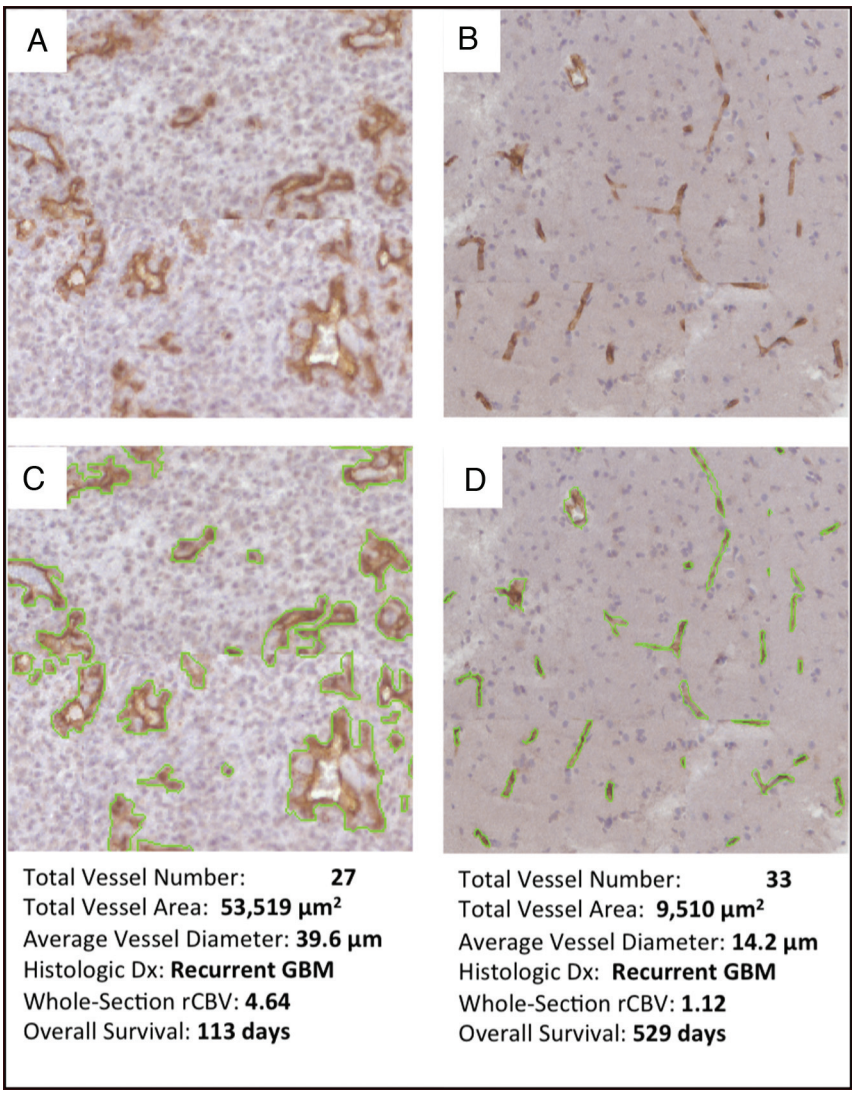

Fig 1. *A* and *B*, Tissue specimens are CD34-stained, as demonstrated in these 2 examples of 0.25-mm^2 microscopic subfields from 2 separate patients with GBM. *C* and *D*, Computer-assisted quantification is used to outline vascular profiles in green. Microvessel parameters, rCBV, and survival were recorded (bottom panel). In this example, the patient with GBM with glomeruloid vessels and corresponding higher vessel area and rCBV (*A* and *C*) demonstrates shorter survival time.

vascular size heterogeneity index, representing the ratio between the SD of the vessel diameter within each sample and the mean vessel diameter. A larger SD relative to vessel size suggests greater heterogeneity of vessel size.[6,7] We selected the index value of 1.0 to yield separation between high (>1) and low (≤ 1) vessel size heterogeneity. Vascular heterogeneity impacted MVD correlations with rCBV; sections with low vascular size heterogeneity showed better correlation between rCBV and MVD ($n = 20$, $r = 0.56$, $P = .01$) compared with the high vascular size heterogeneity group ($n = 18$, $r = 0.20$, $P = .42$). MVA correlation with rCBV remained strong for both high ($r = 0.81$, $P < .001$) and low ($r = 0.82$, $P < .001$) vessel size heterogeneity groups Fig 2.

Microvessel Parameter and rCBV Correlation with OS

At the time of analysis, 12 of 24 subjects had died. One patient who had died had received bevacizumab before imaging and surgery. Bevacizumab has been shown to reduce tissue MVA, MVD, and rCBV values.[22,24,39] Because rCBV represents an imaging measure of tissue microvasculature both in the absence and presence of antiangiogenic therapy,[22] this patient was not excluded from correlations between rCBV, MVA, and MVD as measures of vascularity. However, because bevacizumab does influence the use of MVA, MVD, and rCBV as biomarkers of malignant potential, we excluded this patient from correlations with outcome. Of the patients surviving at the time of analysis, the median time of clinical follow-up was 9.3 months. Cox regression analysis of 23 subjects showed that survival was associated with both MVA ($P = .01$) and rCBV ($P = .02$) but did not reach statistical significance with MVD ($P = .17$). Among this cohort of patients with HGG, histologic grade (III or IV) was associated with survival ($P < .05$).

Discussion

Although histologic grade undoubtedly impacts prognosis, multiple histologic studies have shown that MVA represents an independent predictor of glioma outcome beyond grade alone. Birner et al[8] characterized the microvessel morphometry in 114 GBM (grade IV) tumors, excluding lower grade tumors from analysis. They classified GBM tumors as having

Patient demographic and clinical information[a]				
No.	Age (yr)/Sex	Primary Tumor (grade) No.	RT and Timing (mo completed prior to imaging)	Chemotherapy
1	31/M	AA (III)	60 Gy 3D-C (9) 25 Gy IMRT (2)	T-RT
2	58/M	GBM (IV)	54 Gy 3D-C (22) 12 Gy GK (5)	T-RT
3	36/M	GBM (IV)	60 Gy IMRT (3)	T-RT
4	56/M	GBM (IV)	60 Gy IMRT (23) 30 Gy IMRT (10)	T-RT
5	45/F	GBM (IV)	60 Gy 3D-C (26)	T-RT
6	44/M	GBM (IV)	59.4 Gy IMRT (12)	T-RT
7	50/M	GBM (IV)	37.5 Gy whole-brain RT (8) 30 Gy IMRT (5)	T-RT
8	42/M	GBM (DD-IV)	60 Gy IMRT (60)	T-RT
9	59/M	GBM (IV)	59.4 Gy IMRT (13)	T-RT
10	60/F	Ana. ODG (III)	10 Gy GK (12)	T-RT
11	54/M	AA (III)	59.4 Gy IMRT (11)	T-RT
12	38/M	Ana. GG (III)	54 Gy IMRT (24) 12 Gy GK (11)	T-RT
13	50/M	GBM (IV)	60 Gy IMRT (1)	T-RT
14	42/M	Ana. OA (DD-III)	59.4 Gy IMRT (29)	T-RT
15	25/M	AA (DD-III)	None	None
16	48/F	OA (III)	59.4 Gy 3D-C (76)	T-RT
17	53/M	Ana. ODG (DD-III)	None	None
18	62/F	GBM (IV)	60 Gy 3D-C (8) 12 Gy GK (7)	T-RT
19	25/M	GBM (IV)	60 Gy 3D-C (19)	T-RT & B
20	46/F	Ana. ODG (DD-III)	None	None
21	40/F	AA (III)	None	None
22	49/M	AA (DD-III)	None	None
23	73/F	GBM (IV)	34 Gy IMRT (1)	T-RT
24	34/M	AA (DD-III)	None	None

Note:—AA indicates anaplastic astrocytoma; Ana. GG, anaplastic ganglioglioma; Ana. ODG, anaplastic oligodendroglioma; Ana. OA, anaplastic oligoastrocytoma; DD = dedifferentiated from previous low-grade tumor; IMRT, intensity-modulated radiation therapy; GK, gamma knife; 3D-C, 3D conformal; T-RT, temodar (with initial radiation therapy); B, prior bevacizumab therapy; RT, radiation therapy.

[a] All patients underwent prior surgical treatment for their primary tumors.

the predominance of either glomeruloid vessels (representative of high MVA) or delicate thin-lumen capillary-type vessels (representative of low MVA). Their data showed that GBM tumors lacking glomeruloid vessels were associated with longer patient survival, suggesting that tumoral microvasculature predicts survival differences among tumors with identical histologic grade. Although glomeruloid vessels are considered a histologic hallmark of grade IV tumors, elevated MVA can be observed in grade III tumors as a result of large-area single-lumen microvessels that are not technically considered "glomeruloid."[1,4,8,10] In fact, Korkolopoulou et al[4,10] reported that grade III tumors, even in the absence of glomeruloid vessels, could exhibit MVA that exceeded that of many GBM tumors and supported the findings of Birner et al[8] by showing that elevated MVA was an independent prognostic biomarker of glioma outcome. That MVD may not accurately report the presence of large-area microvessels offers an explanation for why MVD more weakly correlates with outcome compared with MVA.[1,4,8-10]

On the basis of prior histologic studies, it is evident that MVA represents a useful prognostic marker of glioma. Despite its potential value, however, MVA calculation is clinically impractical because of the time-consuming and labor-intensive nature of deriving quantitative measures. Because the calculation of rCBV is both fast and noninvasive compared with that of MVA, a primary goal of the current study was to establish

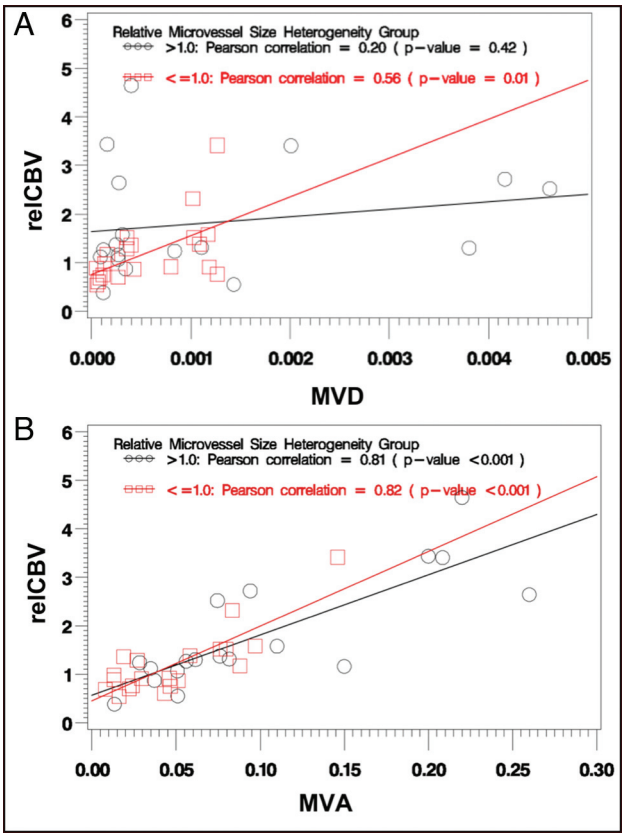

Fig 2. *A,* Measures of rCBV show poor correlation with MVD under conditions of high vessel size heterogeneity ($n = 18$, black data series) but good correlation (red data series) when limiting analysis to homogeneous vessel size ($n = 20$, red series). This "conditional correlation" suggests that rCBV is an unreliable measure of MVD in human HGG, which commonly demonstrates high vessel size heterogeneity. *B,* MVA strongly correlates with rCBV for both high ($n = 18$, black series) and low ($n = 20$, red series) vessel size−heterogeneity groups, suggesting the clinical robustness of rCBV to quantify vessel area in human HGG. Of note, the 6 rightmost data points were measured from 6 different patients.

whether rCBV represents a reliable surrogate of MVA in the clinical setting. We used careful stereotactic coregistration to show that rCBV correlates highly with MVA and generally poorly with MVD. We also showed that the average postprocessing time for rCBV calculation was approximately 5 minutes, compared with approximately 45 minutes for histologic multiparametric microvascular quantification. Knowledge of these histologic correlations provides justification for the use of rCBV as a clinically feasible alternative to tissue MVA quantification as a predictor of glioma outcome.

The results from this study can be compared with those of previous animal work by Pathak et al,[22] who perfused rat 9L gliosarcoma brains with a latex compound (Microfil; Flow Tech, South Windsor, Connecticut) to mark microvessels for histologic area measurement. Although our human tissue specimens demonstrated a comparatively greater range and heterogeneity of vessel sizes ($\leq 125\ \mu m$), the human ($r = 0.83$) and animal ($r = 0.74$) rCBV correlations with MVA remained similarly high, suggesting resilience in the clinical setting. The rCBV correlation with MVA can be explained by the Delesse principle, which states that the "areal attenuation of profiles on sections is an unbiased estimator of the volume attenuation of structures."[22,40] Whereas Pathak et al required correction for thick tissue sections ($50\ \mu m$), our tissue sections ($10\ \mu m$) were substantially thinner. This difference may have improved our correlation. Another difference between the 2 studies is that Pathak et al used MION contrast agent to prevent contrast leakage effects. Because MION is contraindicated in humans, we used preload contrast administration, which robustly minimizes T1-weighted leakage effects, regardless of concomitant steroid therapy.[18,31,32]

In our study, rCBV weakly correlated with MVD within a general population of heterogeneously sized microvessels; however, when the degree of heterogeneity was minimized, rCBV correlation increased. This "conditional correlation" with MVD likely explains the discordance with results from numerous animal tumor models, which generally demonstrate more homogeneous ranges of vessel size compared with human glioma.[21,23-29] Thus, rCBV seems to represent a sufficient measure of MVD (ie, vessel number) in experimental animal models but a poor measure of MVD in the clinical setting. Our results challenge previous clinical reports of high rCBV correlation with MVD in human HGG.[38,41] These discrepancies likely reflect methodologic differences both in imaging-tissue correlation and statistics. For instance, Haris et al[38] did not use spatial coregistration, so regions of rCBV did not necessarily spatially correlate with those of MVD measurement. They chose to match values by rank-order grouping, assuming that high-rCBV locations corresponded to high-MVD locations; this correspondence artificially elevated Pearson correlations. Stereotactic coregistration between imaging-tissue locations in our study precluded the need for rank-order grouping to match values and provided the ability to directly compare rCBV correlations with multiple histologically derived vascular parameters.

Based on conventional theory, the prognostic value of rCBV relates primarily to its prediction of glioma grade, which, in turn, drives clinical outcome.[16-19] However, recent studies have proposed an alternative hypothesis, that rCBV predicts outcome independent of histologic grade.[20,42,43] Law et al[20] and Hirai et al[43] separately reported that rCBV could distinguish survival differences among tumors that were diagnosed histologically as the same grade; however, unlike histology-based studies that correlate MVA and grade within the same tissue sample, none of the imaging-based studies to date have measured rCBV from locations that spatially corresponded with the areas of histologic diagnosis. Thus, these imaging-based studies could not exclude the possibility of sampling errors and histologic misgrading that might influence survival differences within their cohorts.[44]

Our study provides a direct histologic microvascular correlate to rCBV, which helps to support the alternative hypothesis that rCBV can predict survival beyond grade alone.[20,42,43] Specifically, we validate the hypothesis that rCBV reflects tissue MVA, which permits the unification of otherwise separate sources of literature: those studies correlating survival with histologic MVA quantification[1,4,8-10] and those with rCBV measurement.[16,20,42,43] Unlike previous studies that restricted analyses to tumors of identical grade, the size of our cohort was too small to separately assess survival in grade III and grade IV tumors; however, our purpose in this study was not to replicate what has been shown in prior studies. Rather, the goals of our correlation analyses were to uniquely illustrate the following: 1) rCBV and MVA measures, taken from the same

tumor locations, correlated with each other; 2) rCBV and MVA measures, taken from the same tumor locations, correlated similarly with survival; and 3) MVD correlated relatively poorly with both rCBV and survival.

We derived rCBV from a gradient echo–based DSC-MR imaging sequence, which maintains sensitivity to microvessels of all sizes. Other groups have reported spin-echo–based rCBV values, which have a maximal sensitivity to small-diameter microvessels (<25 μm).[16,45,46] In our tissue specimen analysis, many of the large-area microvessels, especially in the GBM, often reached diameters of 75–125 μm. Because spin-echo rCBV values might under-represent these vessel size ranges,[45,46] our choice of gradient-echo DSC-MR imaging seemed appropriate for this study. Future studies by using dual-echo gradient-echo/spin-echo techniques or microvessel tortuosity metrics might help confirm the present findings and also provide insight about microvessel-size heterogeneities.[46,47]

We used the region-of-interest technique primarily for correlative purposes, to enable localized rCBV measurements at locations that corresponded to MVA and MVD quantification from multiple stereotactic biopsies. In our study, the biopsy locations dictated the region-of-interest locations. We do not advocate the application of this method to prospective analysis of DSC-MR imaging data in the absence of biopsy because this would require user-determined random selection of region-of-interest locations. We, instead, would advise consideration of more automated methods of rCBV analysis, such as maximum rCBV or histogram techniques, though comparative studies are likely required, determining which of these methods is most predictive of survival.[20,48]

There are some small measurement differences between rCBV and microvessel area. First, rCBV represented a summation of physiologic and biophysical processes, such as flow dynamics and contrast-tissue interactions, which may have conveyed in vivo microcirculation information differently from histologic structures in isolation.[31,32,47] For example, the presence of hyalinized vessels from prior radiation might confound the correlation between rCBV and microvessel parameters. In general, however, we focused analysis on tissue samples with predominant histologic evidence of tumor, and we excluded from analysis those tissue samples showing predominant radiation effect that might lead to hyalinized vessels. This greatly reduced the presence of hyalinized vessels in our cohort. Second, we performed microvascular analysis from a single representative section for each specimen. Future studies using 3D techniques to quantify microvascular parameters in the entire tissue specimen might improve correlations.[49] Third, we calculated rCBV by normalizing lesion DSC-MR imaging measures with contralateral normal parenchyma, though the tumor specimen microvascular parameters were not similarly normalized. Fourth, we measured rCBV in vivo before surgery and compared it with ex vivo tissue analysis. We, therefore, cannot exclude the effects of anesthesia or surgery on microvessel contractility or possible distortions in microvasculature during tissue treatment (ie, formalin fixation, sectioning, and staining). Future in vivo microscopy studies in humans might refine correlations.[39]

In this study, patients were scanned with either gadodiamide or gadobenate contrast agents, depending on the clinical protocol used by our institution at the time of enrollment. These agents have differing T1 relaxivities, which, theoretically, might become evident through T1-weighted leakage effects and errors in rCBV measurement.[18,31,32,34,46,50] To a large extent, we have greatly minimized these T1-weighted leakage errors through use of preload dosing.[31,34,46] Compared with gadodiamide, gadobenate demonstrates approximately twice the in vivo T1 relaxivity at equivalent doses, which suggests that there would be a greater T1 leakage effect with gadobenate.[50] However, at the same time, the preloading dose of gadobenate may be more effective as well.[31,45] This relationship may be confounded by gadobenate protein binding, which can offset the degree of extravascular contrast extravasation.

Despite the use of different contrast agents in our study, rCBV ultimately demonstrated high correlation with MVA ($r = 0.83$, $P < .0001$). This suggests that preload dosing and DSC-MR imaging are robust techniques and that any residual differences in rCBV estimation that may exist between the contrast agents are unlikely to be clinically significant.

We recognize potential limitations regarding coregistration accuracy between DSC measures and stereotactic locations during open resection.[31,34] Possible discrepancies between imaging region-of-interest size and tissue specimen volumes might have confounded correlation, though we conservatively chose 3×3 voxel regions of interest to roughly correlate with target tissue specimen volumes and to help optimize DSC localization. Image distortions and brain shift following craniotomy could also lead to misregistration errors. To compensate, neurosurgeons used small craniotomy sizes to minimize brain shift and also used visually validated stereotactic image location with intracranial neuroanatomic landmarks to help correct for random brain shifts. Rigid-body coregistration of stereotactic and DSC-MR imaging also helped reduce possible geometric distortions.[51] Overall, our experience suggests combined misregistration at approximately 1–2 mm from both brain shift and registration technique, which is similar to that from previous studies by using stereotactic needle biopsy.[35,36]

Conclusions

We used stereotactic coregistration to demonstrate rCBV as an accurate measure of MVA and propose this correlation as a likely factor in the strong prediction by rCBV of clinical outcome. In contrast, MVD may be a less useful predictor of patient outcome in the clinical setting, compared with MVA or rCBV, and weakly correlates with rCBV due to vascular patterns that cause vessel size heterogeneity.

Acknowledgments

We thank Leslie Dixon, Timothy Pratt, and Lindsay Roberts for their technical assistance with the microvessel quantification for this study.

Disclosures: William R. Shapiro, *Research Support (including provision of equipment or materials)*: EMD Serano, Details: investigator in drug study. Stephen W. Coons, *Consultant*: Global Media, Details: consultant regarding use of GM microscope camera for telepathology. Peter Nakaji, *Consultant*: AlloSource, Aesculap, Medtronic Navigation, Details: cranial bone fusion material, endoscopic surgery teaching, and consultant for image guidance.

References

1. Sharma S, Sharma MC, Sarkar C. **Morphology of angiogenesis in human cancer: a conceptual overview, histoprognostic perspective and significance of neoangiogenesis.** *Histopathology* 2005;46:481–89
2. Schiffer D, Chio A, Mauro GA, et a. **The vascular response to tumor infiltration in malignant gliomas**. *Acta Neuropathol* 1989;77:369–78
3. Abdulrauf SI, Edvardsen K, Ho KL, et al. **Vascular endothelial growth factor expression and vascular density as prognostic markers of survival in patients with low-grade astrocytoma.** *J Neurosurg* 1998;88:513–20
4. Korkolopoulou P, Patsouris E, Kavantzas N, et al. **Prognostic implications of microvessel morphometry in diffuse astrocytic neoplasms.** *Neuropathol Appl Neurobiol* 2002;28:57–66
5. Leon SP, Folkerth RD, Black PM. **Microvessel density is a prognostic indicator for patients with astroglial brain tumors.** *Cancer* 1996;77:362–72
6. Wesseling P, van der Laak JA, Link M, et al. **Quantitative analysis of microvascular changes in diffuse astrocytic neoplasms with increasing grade of malignancy.** *Hum Pathol* 1998;29:352–28
7. Wesseling P, van der Laak JA, de Leeuw H, et al. **Quantitative immunohistological analysis of the microvasculature in untreated human glioblastoma multiforme: computer-assisted image analysis of whole-tumor sections.** *J Neurosurg* 1994;81:902–09
8. Birner P, Piribauer M, Fischer I, et al. **Vascular patterns in glioblastoma influence clinical outcome and associate with variable expression of angiogenic proteins: evidence for distinct angiogenic subtypes.** *Brain Pathol* 2003;13:133–43
9. Folkerth RD. **Histologic measures of angiogenesis in human primary brain tumors.** *Cancer Treat Res* 2004;117:79–95
10. Korkolopoulou P, Patsouris E, Konstantinidou AE, et al. **Hypoxia-inducible factor 1alpha/vascular endothelial growth factor axis in astrocytomas. Associations with microvessel morphometry, proliferation and prognosis.** *Neuropathol Appl Neurobiol* 2004;30:267–78
11. Weidner N, Semple JP, Welch WR, et al. **Tumor angiogenesis and metastasis: correlation in invasive breast carcinoma.** *N Engl J Med* 1991;324:1–8
12. Macchiarini P, Fontaini G, Hardin MJ, et al. **Relation of neovasculature to metastasis of non-small lung cancer.** *Lancet* 1992;340:145–46
13. Hollingsworth HC, Kohn EC, Steinberg SM, et al. **Tumor angiogenesis in advanced stage ovarian carcinoma.** *Am J Pathol* 1995;147:33
14. Bono AV, Celato N, Cova V, et al. **Microvessel density in prostate carcinoma.** *Prostate Cancer Prostatic Dis* 2002;5:123–27
15. Delahunt B, Bethwaite PB, Thornton A. **Prognostic significance of microscopic vascularity for clear cell renal cell carcinoma.** *Br J Urol* 1997;80:401–04
16. Lev MH, Ozsunar Y, Henson JW, et al. **Glial tumor grading and outcome prediction using dynamic spin-echo MR susceptibility mapping compared with conventional contrast-enhanced MR: confounding effect of elevated rCBV of oligodendrogliomas [corrected].** *AJNR Am J Neuroradiol* 2004;25:214–21
17. Knopp EA, Cha S, Johnson G, et al. **Glial neoplasms: dynamic contrast-enhanced T2*-weighted MR imaging.** *Radiology* 1999;211:791–98
18. Boxerman JL, Schmainda KM, Weisskoff RM. **Relative cerebral blood volume maps corrected for contrast agent extravasation significantly correlate with glioma tumor grade, whereas uncorrected maps do not.** *AJNR Am J Neuroradiol* 2006;27:859–67
19. Law M, Yang S, Wang H, et al. **Glioma grading: sensitivity, specificity, and predictive values of perfusion MR imaging and proton MR spectroscopic imaging compared with conventional MR imaging.** *AJNR Am J Neuroradiol* 2003;24:1989–98
20. Law M, Young RJ, Babb JS, et al. **Gliomas: predicting time to progression or survival with cerebral blood volume measurements at dynamic susceptibility-weighted contrast-enhanced perfusion MR imaging**. *Radiology* 2008;247:490–98. Epub 2008 Mar 18
21. Cha S, Johnson G, Wadghiri YZ, et al. **Dynamic, contrast-enhanced perfusion MRI in mouse gliomas: correlation with histopathology.** *Magn Reson Med* 2003;49:848–55
22. Pathak AP, Schmainda KM, Ward BD, et al. **MR-derived cerebral blood volume maps: issues regarding histological validation and assessment of tumor angiogenesis.** *Magn Reson Med* 2001;46:735–47
23. Ali MM, Janic B, Babajani-Feremi A, et al. **Changes in vascular permeability and expression of different angiogenic factors following anti-angiogenic treatment in rat glioma.** *PLoS One* 2010;5:e8727
24. Muruganandham M, Lupu M, Dyke JP, et al. **Preclinical evaluation of tumor microvascular response to a novel antiangiogenic/antitumor agent RO0281501 by dynamic contrast-enhanced MRI at 1.5 T.** *Mol Cancer Ther* 2006;5:1950–57
25. Wilmes LJ, Pallavicini MG, Fleming LM, et al. **AG-013736, a novel inhibitor of VEGF receptor tyrosine kinases, inhibits breast cancer growth and decreases vascular permeability as detected by dynamic contrast-enhanced magnetic resonance imaging**. *Magn Reson Imaging* 2007;25:319–27
26. Hyodo F, Chandramouli GV, Matsumoto S, et al. **Estimation of tumor microvessel density by MRI using a blood pool contrast agent.** *Int J Oncol* 2009;35:797–804
27. Drevs J, Müller-Driver R, Wittig C, et al. **PTK787/ZK 222584, a specific vascular endothelial growth factor-receptor tyrosine kinase inhibitor, affects the anatomy of the tumor vascular bed and the functional vascular properties as detected by dynamic enhanced magnetic resonance imaging.** *Cancer Res* 2002;62:4015–22
28. Badruddoja MA, Krouwer HG, Rand SD, et al. **Antiangiogenic effects of dexamethasone in 9L gliosarcoma assessed by MRI cerebral blood volume maps**. *Neuro Oncol* 2003;5:235–43
29. Doblas S, He T, Saunders D, et al. **Glioma morphology and tumor-induced vascular alterations revealed in seven rodent glioma models by in vivo magnetic resonance imaging and angiography.** *J Magn Reson Imaging* 2010;32:267–75
30. Sorensen AG. **Perfusion MR imaging: moving forward.** *Radiology* 2008;249:416–17
31. Hu LS, Baxter LC, Pinnaduwage DS, et al. **Optimized preload leakage-correction methods to improve the diagnostic accuracy of dynamic susceptibility-weighted contrast-enhanced perfusion MR imaging in posttreatment gliomas.** *AJNR Am J Neuroradiol* 2010;31:40–48
32. Paulson ES, Schmainda KM. **Comparison of dynamic susceptibility-weighted contrast-enhanced MR methods: recommendations for measuring relative cerebral blood volume in brain tumors.** *Radiology* 2008;249:601–13
33. Manka C, Traber F, Gleseke J, et al. **Three-dimensional dynamic susceptibility weighted perfusion MR imaging at 3.0 T: feasibility and contrast agent dose.** *Radiology* 2005;234:869–77
34. Hu LS, Baxter LC, Smith KA, et al. **Relative cerebral blood volume values to differentiate high-grade glioma recurrence from posttreatment radiation effect: direct correlation between image-guided tissue histopathology and localized dynamic susceptibility-weighted contrast-enhanced perfusion MR imaging measurements.** *AJNR Am J Neuroradiol* 2009;30:552–58
35. Stadlbauer A, Ganslandt O, Buslei R, et al. **Gliomas: histopathologic evaluation of changes in directionality and magnitude of water diffusion at diffusion-tensor MR imaging.** *Radiology* 2006;240:803–10
36. Sadeghi N, Salmon I, Decaestecker C, et al. **Stereotactic comparison among cerebral blood volume, methionine uptake, and histopathology in brain glioma.** *AJNR Am J Neuroradiol* 2007;28:455–61
37. Louis DN, Ohgaki H, Wiestler OD, et al., eds. *WHO classification of tumours of the central nervous system.* Lyon, France: IARC; 2002
38. Haris M, Husain N, Singh A, et al. **Dynamic contrast-enhanced derived cerebral blood volume correlates better with leak correction than with no correction for vascular endothelial growth factor, microvascular density, and grading of astrocytoma.** *J Comput Assist Tomogr* 2008;32:955–65
39. Winkler F, Kozin SV, Tong RT, et al. **Kinetics of vascular normalization by VEGFR2 blockade governs brain tumor response to radiation: role of oxygenation, angiopoietin-1, and matrix metalloproteinases.** *Cancer Cell* 2004;6:553–63
40. Weibel ER. *Estimation of Basic Stereologic Parameters: Theoretical Foundations of Stereology*. Vol. 2. London, UK: Academic Press; 1980
41. Liao W, Liu Y, Wang X, et al. **Differentiation of primary central nervous system lymphoma and high-grade glioma with dynamic susceptibility contrast-enhanced perfusion magnetic resonance imaging**. *Acta Radiol* 2009;50:217–25
42. Bisdas S, Kirkpatrick M, Giglio P, et al. **Cerebral blood volume measurements by perfusion-weighted MR imaging in gliomas: ready for prime time in predicting short-term outcome and recurrent disease?** *AJNR Am J Neuroradiol* 2009;30:681–88
43. Hirai T, Murakami R, Nakamura H, et al. **Prognostic value of perfusion MR imaging of high-grade astrocytomas: long-term follow-up study.** *AJNR Am J Neuroradiol* 2008;29:1505–10
44. Jackson RJ, Fuller GN, Abi-Said D, et al. **Limitations of stereotactic biopsy in the initial management of gliomas.** *Neuro Oncol* 2001;3:193–200
45. Young GS, Setayesh K. **Spin-echo echo-planar perfusion MR imaging in the differential diagnosis of solitary enhancing brain lesions: distinguishing solitary metastases from primary glioma.** *AJNR Am J Neuroradiol* 2009;30:575–77
46. Schmainda KM, Rand SD, Joseph AM, et al. **Characterization of a first-pass gradient-echo spin-echo method to predict brain tumor grade and angiogenesis.** *AJNR Am J Neuroradiol* 2004;25:1524–32
47. Kassner A, Annesley DJ, Zhu XP, et al. **Abnormalities of the contrast re-circulation phase in cerebral tumors demonstrated using dynamic susceptibility contrast-enhanced imaging: a possible marker of vascular tortuosity.** *J Magn Reson Imaging* 2000;11:103–13
48. Emblem KE, Nedregaard B, Nome T, et al. **Glioma grading by using histogram analysis of blood volume heterogeneity from MR-derived cerebral blood volume maps.** *Radiology* 2008;247:808–17
49. Gijtenbeek JM, Wesseling P, Maass C, et al. **Three-dimensional reconstruction of tumor microvasculature: simultaneous visualization of multiple components in paraffin-embedded tissue.** *Angiogenesis* 2005;8:297–305
50. Rowley HA, Scialfa G, Gao PY, et al. **Contrast-enhanced MR imaging of brain lesions: a large-scale intraindividual crossover comparison of gadobenate dimeglumine versus gadodiamide.** *AJNR Am J Neuroradiol* 2008;29:1684–91
51. Poetker DM, Jursinic PA, Runge-Samuelson CL, et al. **Distortion of magnetic resonance images used in gamma knife radiosurgery treatment planning: implications for acoustic neuroma outcomes.** *Otol Neurotol* 2005;26:1220–28